

II. New Data and Directions for Neutron Activation Analysis

Richard B. Firestone
Lawrence Berkeley National Laboratory, Berkeley, CA 94720 USA

Lecture presented at the Workshop on Nuclear Data for Activation Analysis,
7-18 March 2005, Trieste, Italy

I. Introduction

In recent years substantial progress has been achieved in the field of Prompt Gamma-ray Activation Analysis (PGAA). The PGAA application also incorporates the use of short-lived activation analysis products. Recently, new precise k_0 measurements for PGAA were performed at the Budapest Reactor. As part of an IAEA CRP, these data were combined with data from the Evaluated Nuclear Structure Data File (ENSDF) and the literature to create the Evaluated Gamma-ray Activation File (EGAF). Much of the data contained in EGAF pertains directly to the k_0 values used in NAA, and there is an opportunity to evaluate the data from both communities to develop better databases for both applications. Additional data needs for Fast Neutron Activation Analysis (FNAA), will also be discussed.

II. Prompt Gamma-ray Activation Analysis (PGAA)

PGAA is a complimentary method to NAA that uses neutron beams to produce prompt γ -rays, following neutron capture, which are used to identify the capturing elements as described in Figure 1.

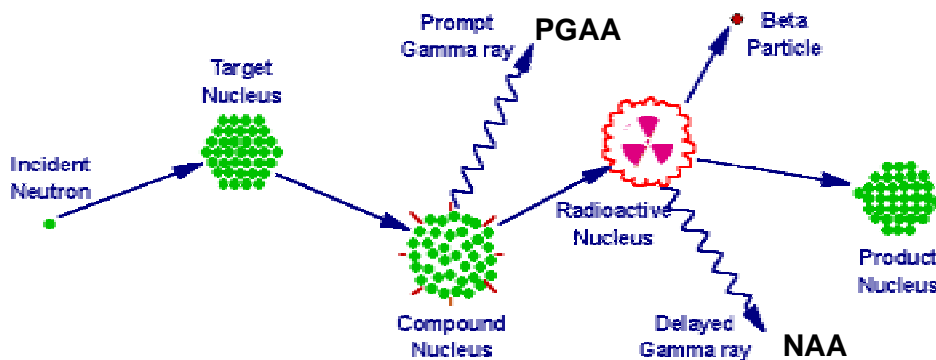


Figure 1. PGAA and NAA

The neutron beams are typically 10^7 n/s, far less than the thermal flux of a reactor, and the emitted γ -ray spectra are usually complex. These limitations are offset by sensitivity to all elements, rapid analysis, and minimal induced radioactivity in the samples. PGAA also uses k_0 analysis techniques and includes short-lived NAA isotopes in its analysis. The γ -rays used in PGAA come from the prompt de-excitation neutron capture state as shown in Figure 2.

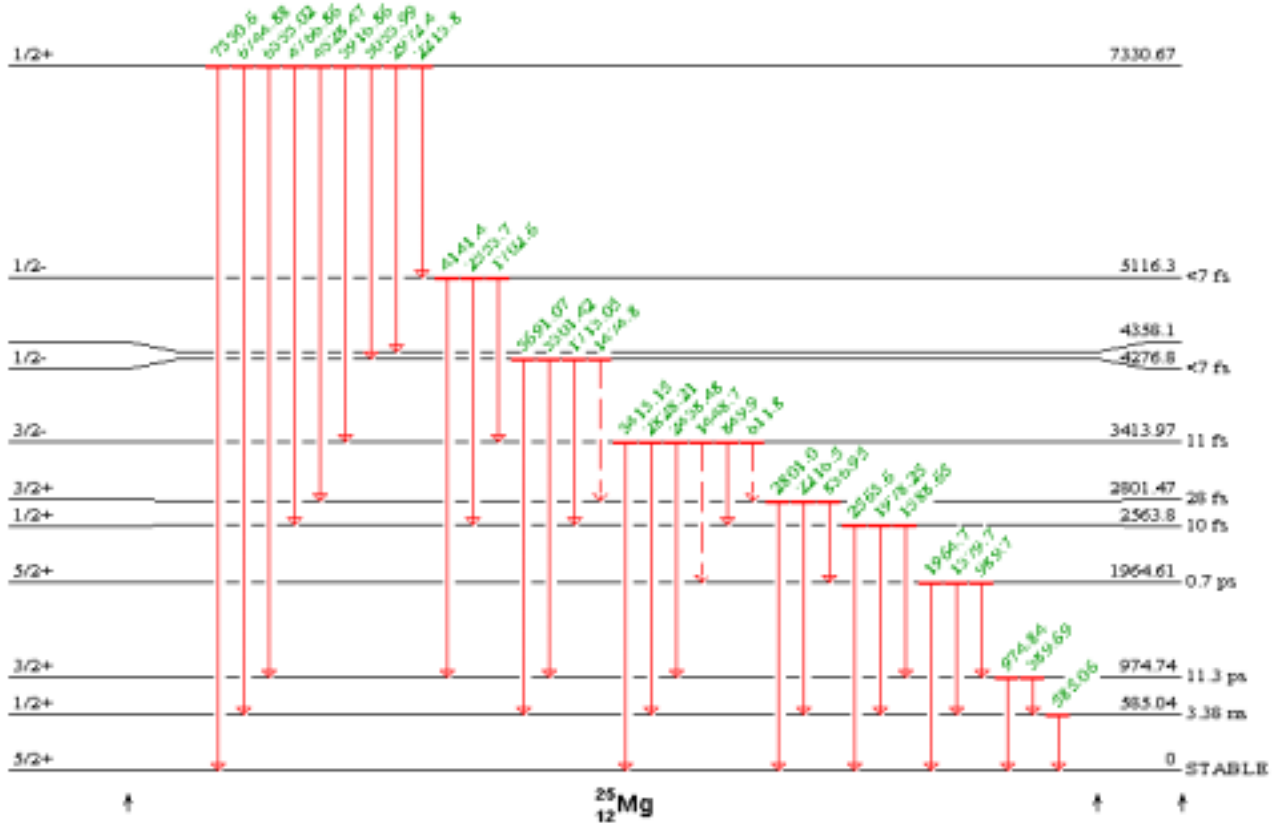
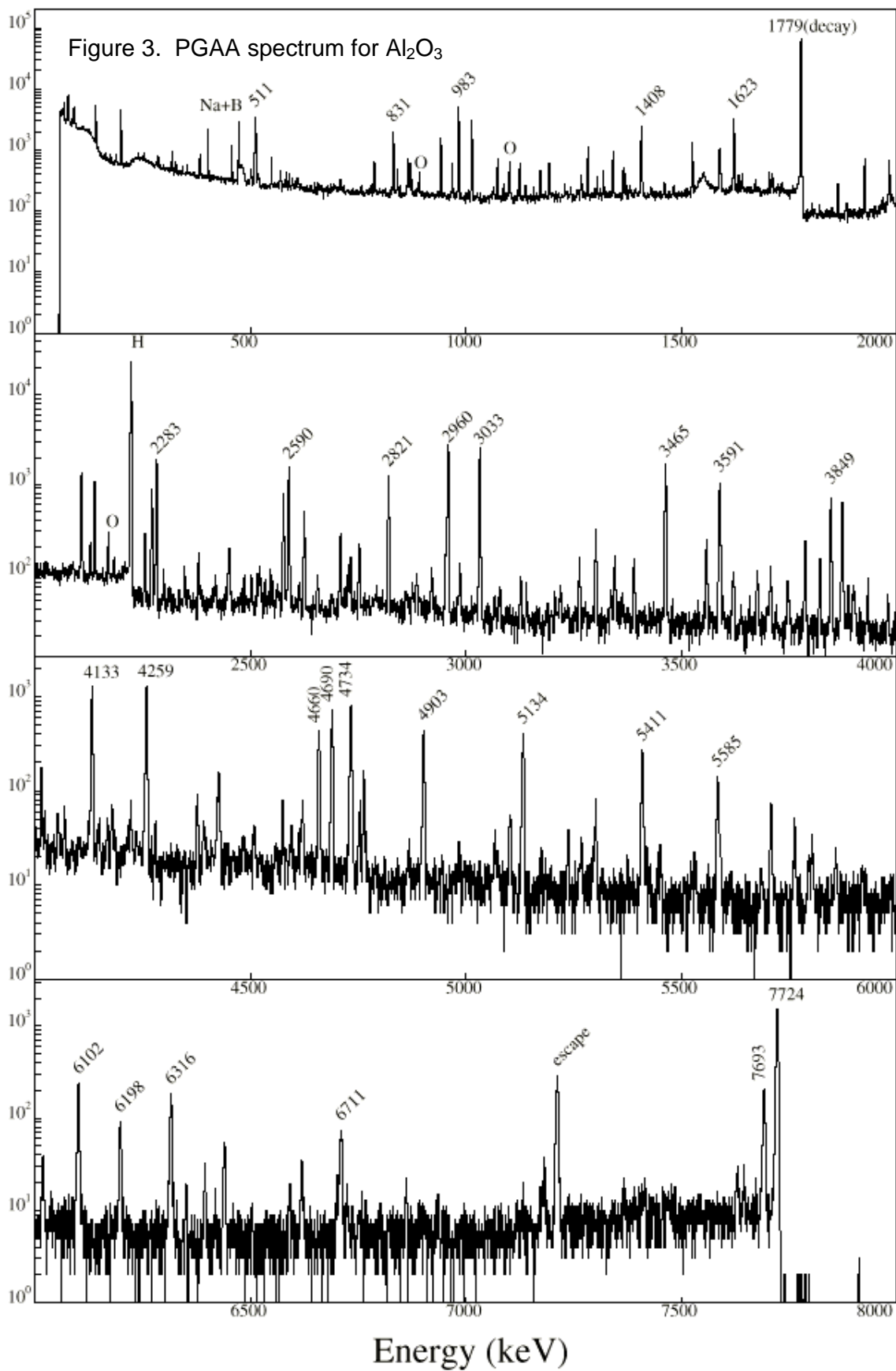


Figure 2. Example of a PGAA neutron capture decay scheme for $^{24}\text{Mg}(n,\gamma)^{25}\text{Mg}$. Unlike NAA, most of the γ -rays are emitted immediately following the neutron capture. Here the primary or initial γ -rays de-excite a capture state at 7330.67 keV producing a cascade of γ -rays to the ground state.

A typical elemental spectrum for aluminum is shown in Figure 3. Note that the 1779-keV γ -ray in this spectrum is from the decay of ^{28}Al (2.24 m). Short-lived isotopes produced by NAA are also used for PGAA. The k_0 value in PGAA is defined similarly to that of NAA where

$$k_0 = M_c \theta_a \sigma_{\gamma a} / M_a \theta_c \sigma_{\gamma c}$$

M_c and M_a are the atomic weights of the comparator and analyte respectively, θ is the isotopic abundance and $\sigma_{\gamma} = P_{\gamma} \sigma_0$ is the partial γ -ray cross section where P_{γ} is the γ -ray transition probability and σ_0 is the total radiative neutron capture cross section.



A. Budapest Reactor Measurements

For many years PGAA was limited by the lack of a well-standardized k_0 database like the one for NAA. Researchers at the Budapest reactor have recently measured k_0 values for nearly all elements from H to U. Capture gamma ray spectra were measured with natural targets using a Compton suppression spectrometer¹. All elemental targets were measured together with a chlorine target in order to achieve a consistent energy calibration. The precise energies of two peaks from the $^{35}\text{Cl}(n, \gamma)$ reaction² were used to determine the energies of two distinct peaks, which were then used for the energy calibration of elemental spectra after non-linearity correction. The accurate new energy and intensity data were sufficient to identify over 13,000 gamma rays from 79 elements.

Measurements with composite targets (stoichiometric compounds, mixtures, or solutions) yielded accurate normalizing factors, with respect to the $\text{H}(n, \gamma)$ cross section, by means of internal k_0 standardization³. Thus, very accurate determinations of the partial gamma-ray production cross-sections and related k_0 -factors became possible. Energies and k_0 -factors for the most important gamma lines have been published^{4,5} and the data library has been discussed^{6,7,8}. Partial cross sections for the best lines for each element were remeasured⁹, often with several targets, and γ -rays from short-lived decay products¹⁰ were included, as summarized in Table I.

B. Evaluated Gamma-ray Activation File (EGAF)

An IAEA CRP was established to evaluate the Budapest data, and other data from the Evaluated Nuclear Structure Data File (ENSDF) and the literature to create a comprehensive database of k_0 and σ_γ values. An IAEA TECDOC containing data for 35,000 γ -ray from 80 elements has been prepared¹¹ is available on the Internet at <http://www-nds.iaea.org/pgaa/>. These data are included in the Evaluated Gamma-ray Activation File (EGAF) which is distributed by the IAEA, and is provided through an interactive data viewer at <http://www-nds.iaea.org/pgaa/pgaa7/index.html>.

1. EGAF Evaluation Methodology

The procedure for evaluation of the EGAF file proceeded as follows.

- a. Create literature and Budapest (n, γ) datasets for each isotope
 - i) Literature dataset from ENSDF, Reedy and Frankel, and the more recent literature (NSR): E_γ , I_γ (per 100 neutron captures)
 - ii) Match the Budapest γ -rays by energy and relative σ_γ to the literature dataset: E_γ , elemental σ_γ (barns)
- b. Combine literature and Budapest datasets into EGAF dataset
 - i) Least-squares fit of γ -ray energies to level scheme with GAMUT.
 - ii) Least-squares fit of γ -ray intensities and cross sections with GAMUT.
 - iii) Evaluate discrepancies and statistical outliers.
 - iv) Create EGAF data file: E_γ , elemental σ_γ , normalization to isotopic σ_γ
- c. Test EGAF level scheme γ -ray intensity balance.
 - i) Check the level scheme intensity balance
 - ii) Compare the total GS γ -ray feedings with BNL-325.

Table I. Partial γ -ray cross sections for the elements as measured by internal standardization at the Budapest thermal guide⁹. Decay gamma rays are denoted by d in the energy column.

Z	El	E_{γ} -keV	$\sigma_{\gamma}^Z(E_{\gamma})$ -	Z	El	E_{γ} -keV	$\sigma_{\gamma}^Z(E_{\gamma})$ -
1	H	2223.2590(10)	0.3326(7)	54	Xe	667.87(9)	6.9(10)
3	Li	2032.300(20)	0.038(1)	55	Cs	5505.46(20)	0.306(4)
4	Be	6809.58(10)	0.0054(5)	56	Ba	1435.65(6)	0.308(6)
5	B	478(3)	713(5)	57	La	567.413(23)	0.333(7)
6	C	1261.71(6)	0.00120(2)	58	Ce	662.03(5)	0.233(18)
		4945.30(7)	0.00262(3)	59	Pr	176.95(3)	1.06(2)
7	N	1884.85(3)	0.01458(6)	60	Nd	696.487(20)	33.2(7)
8	O	870.68(3)	0.000175(8)	62	Sm	334.02(5)	4900(60)
9	F	1633.53(3)d	0.0093(3)	63	Eu	89.97(8)	1450(20)
11	Na	472.222(13)	0.497(5)	64	Gd	182.12(6)	7680(170)
12	Mg	584.936(24)	0.0327(7)	65	Tb	74.89(8)	0.35(4)
13	Al	1778.92(3)d	0.233(4)	66	Dy	184.34(7)	146(3)
14	Si	3538.98(5)	0.119(2)	67	Ho	136.67(4)	14.5(7)
15	P	636.570(17)	0.031(1)	68	Er	184.301(25)	57(2)
16	S	841.013(14)	0.357(7)	69	Tm	204.41(5)	8.7(1)
17	Cl	1951.150(15)	6.51(4)	70	Yb	639.73(3)	1.5(1)
19	K	770.325(23)	0.91(2)	71	Lu	150.34(6)	13.7(4)
20	Ca	1942.68(3)	0.34(1)	72	Hf	213+214	1.97(4)
21	Sc	584.80(3)	1.83(3)	73	Ta	270.48(6)	2.60(4)
22	Ti	1381.74(3)	5.18(5)	74	W	145.74(9)	0.97(2)
23	V	1434.10(3)d	5.2(1)	75	Re	207.92(4)	4.5(2)
24	Cr	834.80(3)	1.38(2)	76	Os	186.85(3)	2.08(4)
25	Mn	846.829(1)d	13.3(2)	77	Ir	351.59(5)	2.42(8)
26	Fe	7631.05(9)	0.68(1)	78	Pt	355.54(4)	6.17(5)
27	Co	229.811(12)	7.18(7)	79	Au	215.01(3)	7.77(5)
28	Ni	464.972(18)	0.843(9)	80	Hg	5967.00(10)	53(2)
29	Cu	277.993(25)	0.893(9)	81	Tl	873.16(8)	0.168(6)
30	Zn	1077.336(17)	0.358(4)	82	Pb	7367.83(12)	0.137(3)
31	Ga	690.943(24)	0.26(3)	83	Bi	319.83(4)	0.017(2)
32	Ge	595.879(20)	1.59(4)	90	Th	256.25(11)	0.093(4)
33	As	165.09(3)	1.00(1)	92	U	4060.35(5)	0.186(3)
34	Se	6600.67(12)	0.57(3)				
35	Br	1248.78(12)	0.054(1)				
37	Rb	556+557	0.132(2)				
38	Sr	1836.05(3)	1.02(1)				
39	Y	6080.12(7)	0.85(2)				
40	Zr	213+214	0.125(6)				
41	Nb	499.48(3)	0.065(5)				
42	Mo	778.221(10)	2.04(5)				
44	Ru	539.522(11)	1.5(1)				
45	Rh	470.41(3)	2.50(7)				
46	Pd	616.219(15)	0.638(6)				
47	Ag	657.741(22)	1.93(4)				
48	Cd	558.32(3)	1866(21)				
49	In	5892.38(15)	2.1(2)				
50	Sn	1293.53(6)	0.134(2)				
51	Sb	921.04(4)	0.086(4)				
52	Te	602.723(12)	2.4(2)				
53	I	133.59(4)	1.42(5)				

An example of the least squares energy fit is shown in Table 2.

ENSDF	Budapest	Adopted	Level-1	Level-2
389.69 5	(1)389.64 3	389.685 18	3	2
(2)585.06 3	(2)584.936 24	584.994 16	2	1
611.8 10		611.80 9	7	6
(1)836.95 10	836.75 8	836.82 6	6	4
849.9 3	849.93 16	850.01 3	7	5
(2)863.09 5	(2)862.88 4	862.962 23	8	7
(3)974.84 5	(1)974.61 3	974.669 18	3	1
989.7 4		989.98 9	4	3
1379.7 3	1379.69 19	1379.65 9	4	2
1448.7 10		1448.61 9	7	4
1474.8 10		1474.74 9	8	6
1588.65 9	(1) 1588.40 9	1588.58 3	5	3
-	-	-	-	-
-	-	-	-	-
3691.07 16	3690.98 18	3691.03 3	8	2
3916.86 4	(1)3916.65 16	3916.85 3	11	7
4141.4 3	4141.38 24	4141.31 14	10	3
	4357.9 6	4357.8 5	9	1
4528.47 20	4528.66 22	4528.55 9	11	6
4766.86 23	4766.68 25	4766.71 4	11	5
6355.02 10	6354.9 3	6354.96 3	11	3
(1)6744.9 3		6744.54 3	11	2
(1)7330.6 9		7329.37 3	11	1
Level	Energy		Level	Energy
1.	0.0		7.	3413.341 23
2.	585.001 16		8.	4276.32 3
3.	974.689 18		9.	4358.2 5
4.	1964.69 9		10.	5116.36 14
5.	2563.32 3		11.	7330.52 3
6.	2801.53 9			

Table 2. First iteration of a least squares fit of gamma-ray energies to the level scheme for $^{24}\text{Mg}(n,\gamma)$. The numbers in parentheses represent the discrepancy in the number to the right, compared to the adopted value, expressed in terms of the number of standard deviations. The uncertainties in each dataset were increased and additional iterations were performed until $\chi^2/\text{f} = 1$.

Table 3 shows the a similar least squares fit of the γ -ray intensities.

GAMMA ENERGIES	FITTED INTENSITIES				
	1. 24MG(N,G)		2. 24MG(N,G)		
389.699 20	7.5 4	7.5 3	5.8 3	5.82 25	18.3 7
584.9360 20	39.8 12	40.0 11	31.6 15	31.2 12	98.1 25
611.79 9	0.015 15	0.015 15	0.0	0.012 12	0.04 4
836.82 6	0.21 3	0.201 19	0.152 18	0.157 15	0.49 5
849.98 4	0.070 20	0.085 14	0.072 15	0.066 11	0.21 4
974.625 20	8.3 4	8.3 4	6.2 9	6.4 4	20.3 9
989.98 9	0.050 10	0.050 10	0.0	0.039 8	0.123 25
1379.67 9	0.100 20	0.108 14	0.088 14	0.084 11	0.26 3
1448.59 9	0.015 15	0.015 15	0.0	0.012 12	0.04 4
1474.74 9	0.015 15	0.015 15	0.0	0.012 12	0.04 4
1588.59 4	0.37 5	0.32 3	0.222 25	0.248 22*1*	0.78 7
1703.13 16	0.040 10	0.040 10	0.0	0.031 8	0.098 25
1712.92 4	1.8 3	1.55 10	1.18 7	1.20 7	3.79 21
1964.57 9	0.06 4	0.104 23*1*	0.085 20	0.081 18	0.26 6
1978.26 3	1.42 11	1.41 7	1.10 6	1.10 5	3.47 15
2213.89 16	0.40 5	0.38 4	0.23 5	0.29 3*1*	0.92 10
2216.44 9	0.25 4	0.23 3	0.13 4	0.18 3*1*	0.57 8
2438.513 25	6.3 4	6.0 3	4.59 22	4.71 20	14.8 6
2553.05 16	0.030 10	0.030 10	0.0	0.023 8	0.074 25
2563.15 3	0.070 20	0.070 20	0.0	0.055 16	0.17 5
2801.32 9	0.170 20	0.167 19	0.08 4	0.130 16*1*	0.41 5
2828.171 25	30.5 10	30.6 9	23.9 11	23.8 9	74.9 20
2972.1 6	0.090 20	0.090 20	0.0	0.070 18	0.22 5
3053.99 3	10.4 5	10.5 4	8.3 4	8.2 3	25.8 9
3301.40 3	7.7 4	7.9 3	6.3 3	6.16 25	19.4 7
3413.036 25	5.1 3	5.12 22	4.00 20	3.99 17	12.6 5
3691.04 3	0.90 8	0.87 6	0.65 6	0.68 5	2.13 14
3916.85 3	41.0 13	40.8 12	31.4 15	31.8 12	100 3
4141.46 16	0.21 3	0.196 20	0.142 20	0.153 16	0.48 5
4357.8 6	0.0	0.0	0.0	0.0	0.0
4528.54 9	0.46 4	0.44 4	0.29 5	0.34 3*1*	1.08 8
4766.69 4	0.41 4	0.42 3	0.33 3	0.325 22	1.02 7
6354.95 3	1.31 9	1.35 7	1.09 8	1.05 6	3.31 17
6744.55 3	0.18 3	0.18 3	0.0	0.140 25	0.44 7
7329.31 3	0.018 4	0.018 4	0.0	0.014 3	0.044 9
CHI/F	0.1716570		0.3695236		
SKEW	0.1544303		-1.4765821		
NDEGREES	34		24		

Table 3. Fit of γ -ray intensities measured at Budapest (set 1) and from the literature (set 2). A normalization factor is determined for each data set by least-squares minimization of the uncertainty in the average of all pairs of values.

Intensity data are checked by inspection of the intensity balance through the capture gamma decay scheme as shown in Table 4.

Table 4. Intensity balance in barns from EGAF data for $^{24}\text{Mg}(n,\gamma)^{25}\text{Mg}$. The intensity de-exciting the capture state should equate the intensity feeding the ground state, and there should be no net feeding to intermediate levels. Note the excellent agreement between net primary and secondary g-ray cross-sections and the values compiled by Mughabghab.

E(Level)	$\sigma(\text{in})$	$\sigma(\text{out})$	$\Delta\sigma$
0	0.0536(14)	0.0	0
585.01(3)	0.0406(11)	0.0398(14)	0.0008(18)
974.68(3)	0.0157(4)	0.0158(4)	0.0001(6)
1964.69(10)	0.00022(2)	0.00026(3)	0.00004(4)
2563.35(4)	0.00202(10)	0.00179(7)	0.00023(12)
2801.54(9)	0.00047(4)	0.00061(5)	0.00013(6)
3413.35(3)	0.0411(14)	0.0416(11)	0.0005(18)
4276.33(4)	0.0105(4)	0.0107(3)	0.0002(5)
4358.2(5)	0.00009(2)	0.0	0.00009(2)
5116.37(15)	0.00038(4)	0.00027(3)	0.00011(5)
7330.53(4)	0.0	0.0539(14)	0.0539(14)
$\sigma(\text{Mughabghab}[23])$		0.0536(15) b	
$\sigma(\text{Measured, average})$		0.0538(14) b	

The IAEA website provides EGAF data with a periodic table interface, similar to that of the k0 website, as shown in Figure 4. Selection of an element gives a list of isotopes for that element, and data for each isotope can be displayed in a histogram, as in Figure 5, or a table as in Table 5. EGAF data can also be searched on-line from the IAEA EGAF website as shown in Figure 6 and Table 6.



PGAA

Prompt Gamma-ray Neutron Activation Analysis

This database has been developed as part of a Coordinated Research Project for the Development of a Database for Prompt Gamma-ray Neutron Activation Analysis sponsored by the International Atomic Energy Agency (IAEA). The data are derived from the isotopic measurements compiled in the Evaluated Nuclear Structure Data File (ENSDF), updated when necessary, and from elemental measurements performed at the Budapest Reactor Centre. The data were received from Richard B. Firestone (Lawrence Berkeley National Laboratory, USA). The program "Viewer" was developed by Viktor Zerkov (IAEA, NDS).

PGAA: Target Elements and Isotopes

Selected Element

82-Lead (64)
Pb-204 (35)
Pb-206 (6)
Pb-207 (23)

1 H																	2 He
3 Li	4 Be											5 B	6 C	7 N	8 O	9 F	10 Ne
11 Na	12 Mg											13 Al	14 Si	15 P	16 S	17 Cl	18 Ar
19 K	20 Ca	21 Sc	22 Ti	23 V	24 Cr	25 Mn	26 Fe	27 Co	28 Ni	29 Cu	30 Zn	31 Ga	32 Ge	33 As	34 Se	35 Br	36 Kr
37 Rb	38 Sr	39 Y	40 Zr	41 Nb	42 Mo	Tc	44 Ru	45 Rh	46 Pd	47 Ag	48 Cd	49 In	50 Sn	51 Sb	52 Te	53 I	54 Xe
55 Cs	56 Ba	57* La	72 Hf	73 Ta	74 W	75 Re	76 Os	77 Ir	78 Pt	79 Au	80 Hg	81 Tl	82 Pb	83 Bi	Po	85 At	86 Rn
87 Fr	88 Ra	89** Ac	104 Rf	105 Db	106 Sg	107 Bh	108 Hs	109 Mt	110 *	111 *	112 *						
* Lanthanides			58 Ce	59 Pr	60 Nd	61 Pm	62 Sm	63 Eu	64 Gd	65 Tb	66 Dy	67 Ho	68 Er	69 Tm	70 Yb	71 Lu	
** Actinides			90 Th	91 Pa	92 U	93 Np	94 Pu	95 Am	96 Cm	97 Bk	98 Cf	99 Es	100 Fm	101 Md	102 No	103 Lr	

Database Search:

▪ [from smaller version of database](#)

▪ [from full database](#)

(see: [limitations](#))

Display:

▪ [Table of elements](#)

▪ [Table of elements & isotopes](#)

Download:

▪ [PGAA data as plain text](#)

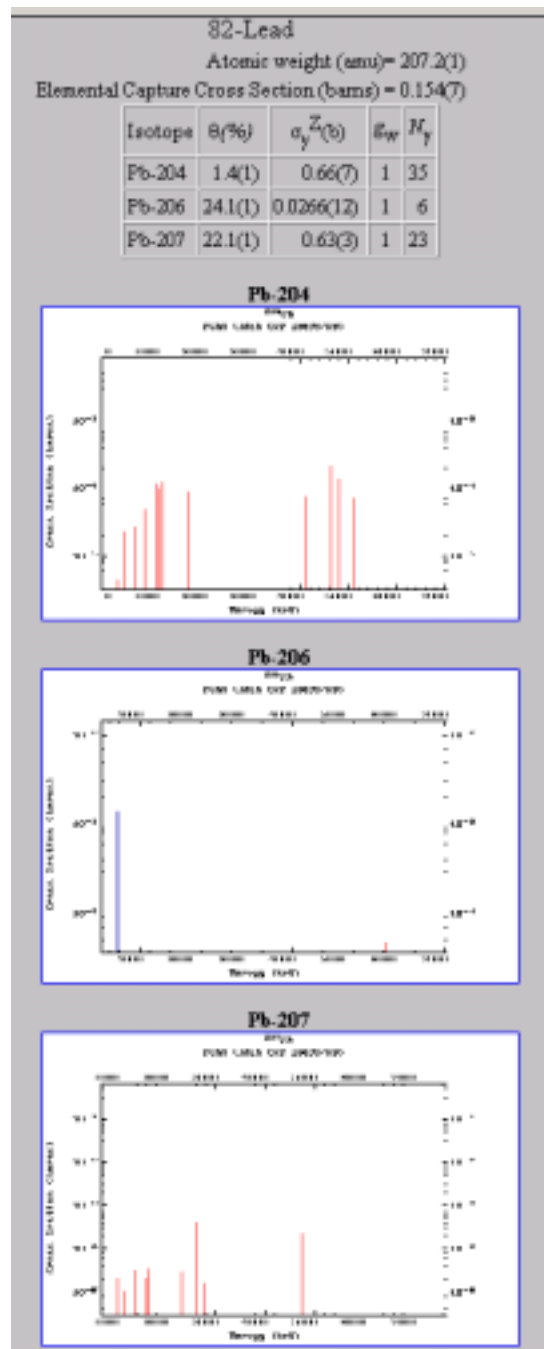
▪ [Adopted Gamma Rays for Elements program](#)

▪ [Most Intense Gamma Rays](#)

Link:

▪ [ZVView: plotting](#)

Figure 4. Selection of an element from the periodic table provides a list of isotopes whose data can be displayed.




82-Lead-207
Isotopic Abundance(%) 22.1(1)
Isotopic Capture Cross Section (barns): 0.63(3)
Number of Gammas: 23
Westcott g-factor: 1

#	$E_{\gamma}(keV)$	$\sigma_{\gamma}^Z(b)$	Type	Half-life	k_0
1	1025(3)	2.2E-05(5)	p	Stable	3.2E-07(7)
2	1155.06(16)	1.10E-05(19)	p	Stable	1.6E-07(3)
3	1332.82(19)	5E-06(3)	p	Stable	7E-08(4)
4	1383(4)	3.3E-05(7)	p	Stable	4.8E-07(10)
5	1437.40(17)	8E-06(3)	p	Stable	1.2E-07(4)
6	1523.36(19)	1.1E-05(3)	p	Stable	1.6E-07(4)
7	1615.16(16)	2.2E-05(3)	p	Stable	3.2E-07(4)
8	1640.17(8)	3.6E-05(4)	p	Stable	5.3E-07(6)
9	1983.13(15)	3.8E-05(8)	p	Stable	5.6E-07(12)
10	2086.8(21)	3.8E-05(8)	p	Stable	5.6E-07(12)
11	2322.62(8)	3.0E-05(4)	p	Stable	4.4E-07(6)
12	2430.72(8)	3.0E-05(4)	p	Stable	4.4E-07(6)
13	2614.53(3)	0.00040(3)	p	Stable	5.9E-06(4)
14	2770.21(15)	1.6E-05(3)	p	Stable	2.3E-07(4)
15	3113.17(8)	3.6E-05(6)	p	Stable	5.3E-07(9)
16	3282.39(7)	8.5E-05(9)	p	Stable	1.24E-06(13)
17	3729(3)	2.2E-05(11)	p	Stable	3.2E-07(16)
18	4085.46(7)	1.04E-04(17)	p	Stable	1.52E-06(25)
19	4753.31(7)	2.33E-04(17)	p	Stable	3.41E-06(25)
20	4937.12(8)	2.5E-05(25)	p	Stable	4E-07(4)
21	5384.71(15)	8E-06(3)	p	Stable	1.2E-07(4)
22	5844.46(20)	1.4E-05(4)	p	Stable	2.0E-07(6)
23	7367.78(7)	0.137(3)	p	Stable	0.00200(4)

p - Prompt, d - Delayed

Figure 5

*Nuclear
Data
Service*



International Atomic Energy Agency

P G A A

Advanced Retrieval: Full Version

Gamma-Ray Search

	Energy (keV)	Z	A	CS(b)
From	<input checked="" type="checkbox"/> 2000	<input checked="" type="checkbox"/> 1	<input checked="" type="checkbox"/> 1	<input checked="" type="checkbox"/> 0
To	<input checked="" type="checkbox"/> 2002	<input checked="" type="checkbox"/> 92	<input checked="" type="checkbox"/> 238	<input checked="" type="checkbox"/> 100

Type: ☒ All ☐ Prompt ☐ Delayed
 Sort by: ☒ Energy ☐ Cross Section

Figure 6. EGAF retrieval menu.

- P G A A -

n	E_γ, keV	Isotope	$\sigma_\gamma^2(E_\gamma), \text{b}$	Type	Half-life	k_0
1	2000.10(3)	Ge-76	6.67E-05(13)	d	11.30 h	2.78E-06(6)
2	2000.30(20)	Xe-136	2.02E-06(21)	d	3.818 m	4.7E-08(5)
3	2000.4(9)	Ti-46	0.0009(3)	p	S	5.7E-05(19)
4	2000.639(3)	Er-167	0.10(5)	p	S	0.0018(9)
5	2000.73(4)	K-39	0.0018(4)	p	S	1.4E-04(3)
6	2000.9(8)	Zn-70	2.0E-09(5)	d	3.96 h	9.3E-11(24)
7	2000.94(6)	Te-130	1.87E-04(5)	d	30 h	4.44E-06(12)
8	2001.05(5)	Cr-50	0.0199(10)	p	S	0.00116(6)
9	2001.31(3)	Ca-40	0.0659(15)	p	S	0.00498(11)
10	2001.4(3)	Nb-93	0.0025(6)	p	S	8.2E-05(20)
11	2001.70(8)	Sn-115	2.0E-04(8)	p	S	5.1E-06(20)
12	2001.920(19)	N-14	1.9E-04(4)	p	S	4.1E-05(9)

p - Prompt, d - Delayed, S - Stable

Table 6. Results of retrieval.

C. Determination of k_0 values from EGAF

The PGAA k_0 values in EGAF were calculated with respect to the comparator hydrogen. They can easily be converted to other standards dividing by the k_0 of the standard γ -ray of interest. For conversion to $^{198}\text{Au}(411.8\gamma)$ standardization, the conversion factor is 94.29(15) barns. There are about 3000 k_0 values for decay (NAA) gammas in EGAF. The 1779-keV ^{28}Al decay γ -ray, discussed earlier, gives $k_0(\text{PGAA})=0.0180(4)$ which agrees well with $k_0=0.0175$ from the k_0 website.

The total radiative cross-section σ_0 can also be derived for many cases where the neutron capture decay scheme is sufficiently complete, as was shown for $^{23}\text{Mg}(n,\gamma)$ earlier. In this case the k_0 value can be determined from the decay scheme data available in the Evaluated Nuclear Structure Data File (ENSDF)¹³ and other evaluations. A simple example is shown in Figure 7 for the reaction $^{63}\text{Cu}(n,\gamma)^{64}\text{Cu}(12.7\text{ h})$.

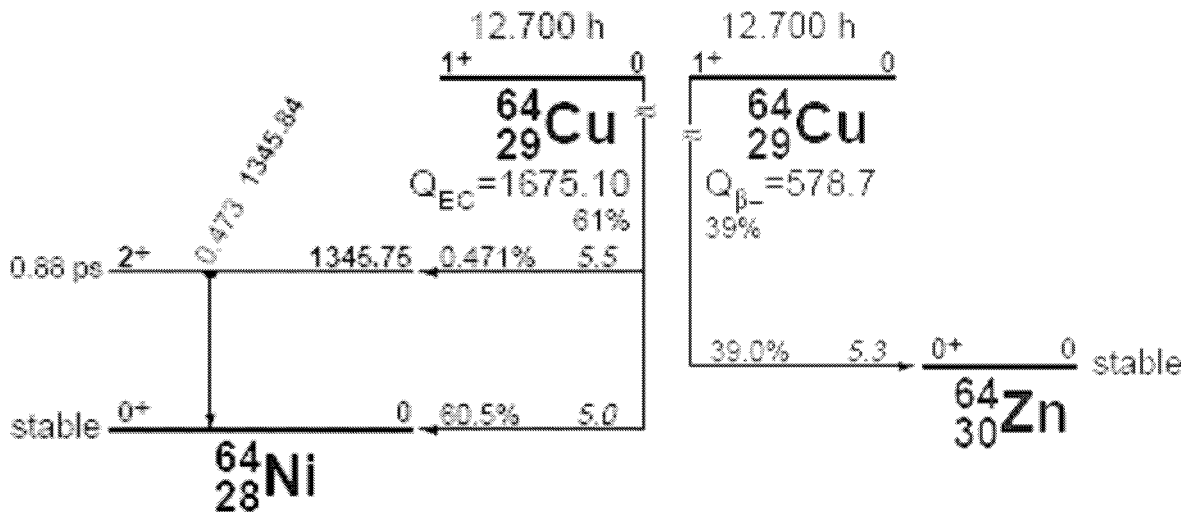


Figure 7. EC and β^- decay schemes for ^{64}Cu from the Table of Isotopes¹⁴.

The most recent recommended transition probability for the 1345.8 keV γ -ray from ^{64}Cu EC decay $P_{1346}=0.475(10)$ ¹⁵. From the EGAF σ_γ data we have derived $\sigma_0(^{63}\text{Cu})=4.75(4)$ b, somewhat greater than the standard value 4.52(2) b of Mughabghab¹⁶. As discussed earlier

$$\begin{aligned}
 k_0 &= M_c \theta_a P_{\gamma a} \sigma_{0a} / M_a \theta_c P_{\gamma c} \sigma_{0c} \\
 &= 196.96655 \times 0.6917 \times 0.00475 \times \sigma_0 / (63.546 \times 1 \times 0.9554 \times 98.65) \\
 &= 5.13(5) \times 10^{-4} \text{ (EGAF)} \\
 &= 4.88(3) \times 10^{-4} \text{ (Mughabghab)} \\
 &= 4.91 \times 10^{-4} \text{ (} k_0 \text{ webpage)}
 \end{aligned}$$

The results are discrepant suggesting that a new evaluation including all of the available data will improve the values in the EGAF, NAA, and decay databases. Table 7 lists a comparison of k_0 values derived from EGAF with those in the k_0 website.

Table 7. Comparison of Internet k_0 values of Blaauw with values derived from the EGAF database.

Element	E_γ	$k_0(\text{WWW})$	$k_0(\text{EGAF})$	Element	E_γ	$k_0(\text{WWW})$	$k_0(\text{EGAF})$
Na	1368.7	4.68E-02	0.0481(13)	Cs	127.5	5.48E-03	4.89(16)E-03
	2754.1	4.62E-02	0.0481(13)	Ba	165.9	1.05E-03	1.12(13)E-03
Mg	843.7	2.53E-04	2.56(10)E-04	La	328.8	2.87E-02	1.88(4)E-02
Al	1778.9	1.75E-02	0.0180(4)		432.5	4.20E-03	2.67(8)E-03
Si	1266.2	1.73E-07	1.9(3)E-07		487.0	6.37E-02	4.19(11)E-02
Cl	2166.9	2.66E-03	3.34(10)E-03		751.6	6.19E-03	3.98(8)E-03
K	1524.6	9.46E-04	1.07(2)E-03		815.8	3.32E-02	2.15(5)E-02
Ca	3084.4	1.01E-04	9.9(10)E-05		1596.2	1.34E-01	0.088(3)
Ti	320.1	3.74E-04	3.74(4)E-4	Pr	1575.6	6.12E-03	6.33(20)e-03
V	1434.1	1.96E-01	0.197(4)	Nd	211.3	5.26E-04	5.37(21)E-04
Mn	846.8	4.96E-01	0.0497(10)	Sm	104.3	1.79E-02	0.0198(6)
Ni	1481.8	1.27E-04	1.17(3)E-04	Gd	360.9	2.72E-03	2.64(8)E-03
Cu	1039.0	1.86E-03	1.96(5)E-03	Dy	108.2	1.88E-01	0.175(8)
Zn	438.6	3.98E-04	4.08(17)E-04	Ho	80.6	5.45E-02	0.0489(14)
As	559.1	4.83E-02	5.6(3)E-02	Yb	113.8	9.42E-03	5.0(3)E-03
	657.0	6.61E-03	7.8(4)E-03		282.5	1.46E-02	0.0081(3)
	1216.1	3.78E-03	4.3(2)E-03		396.3	3.12E-02	0.0171(7)
Br	554.3	2.38E-02	0.0221(3)	Lu	113.0	3.63E-02	0.0413(22)
	619.1	1.45E-02	0.0134(2)		208.4	6.05E-02	0.072(4)
	698.4	9.38E-03	8.80(17)E-03	Hf	214.3	1.61E-01	0.191(5)
	776.5	2.76E-02	0.0258(6)	Ta	171.6	5.84E-05	6.22(13)E-05
	827.8	7.99E-03	7.44(15)E-03	W	134.2	1.13E-02	0.0119(4)
Rb	1076.6	7.65E-04	7.34(15)E-04		479.6	2.97E-02	0.0294(8)
Sr	388.5	1.49E-03	1.87(6)E-03		551.5	6.91E-03	6.84(20)E-03
Ru	724.3	8.87E-04	1.84(4)E-03		618.3	8.65E-03	8.5(3)e-03
Rh	51.5	7.43E-02	0.0105(6)		625.5	1.48E-03	1.47(5)E-03
Ag	657.5	3.44E-02	0.0360(11)		685.7	3.71E-02	0.0367(11)
In	138.3	1.01E-01	0.093(3)		772.9	5.61E-03	5.56(17)E-03
	416.9	7.54E-01	0.778(23)	Re	137.2	4.33E-02	0.0592(18)
	818.7	3.36E-01	0.323(13)		155.0	7.77E-02	0.080(3)
	1097.3	1.60E+00	1.58(3)	Ir	293.5	2.03E-02	0.0191(8)
	1293.5	2.29E+00	2.38(3)		328.4	1.03E-01	0.098(4)
	1507.4	2.69E-01	0.281(8)	Au	411.8	1.00E+00	1.000(2)
	1753.8	6.67E-02	0.070(2)	U	106.1	6.19E-03	6.33(13)E-03
	2112.1	4.18E-01	0.437(13)		209.8	7.80E-04	7.96916)E-04
Sn	331.9	1.18E-04	1.46(5)-04		228.2	2.77E-03	2.51(8)E-03
Sb	564.2	4.38E-02	0.0462(9)		277.6	3.40E-03	3.34(7)E-03
	692.6	2.38E-03	2.50(10)E-03		315.9	3.68E-04	3.72(8)E-04
In	442.9	1.12E-02	0.0096(2)		334.3	4.81E-04	4.82(10)e-04

III. Activation Analysis with Neutron Generators

Neutron generators offer the possibility of doing activation analysis away from reactors in small laboratories. New designs promise fast neutron rates of 10^{12} (D+D, 2.5 MeV) to 10^{14} (D+T, 14 MeV) n/s¹⁷. Figure 8 shows the 10^{10} n/s D+D neutron generator facility at LBNL.

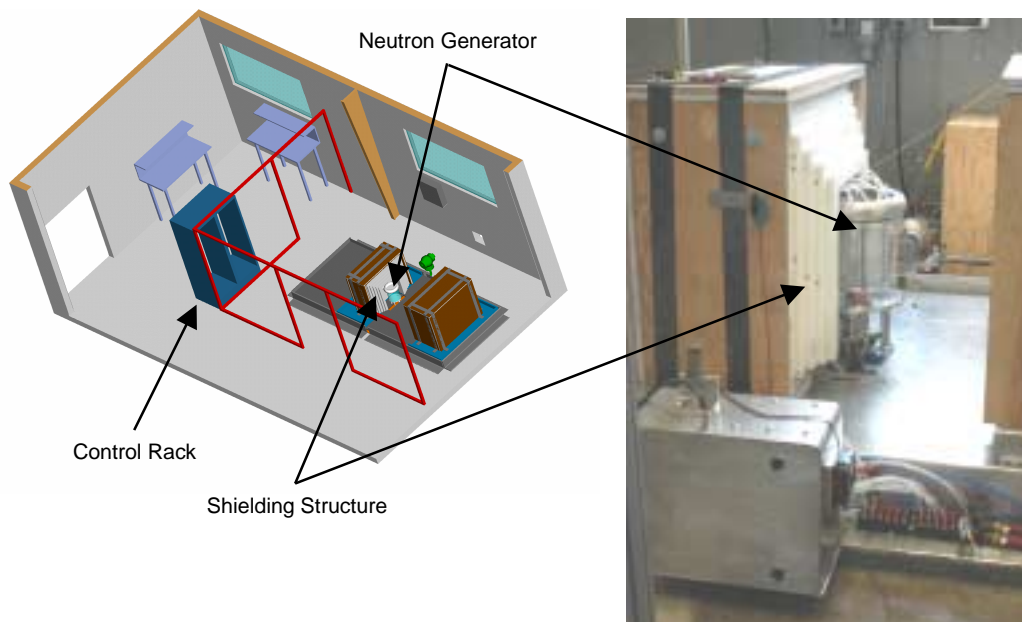
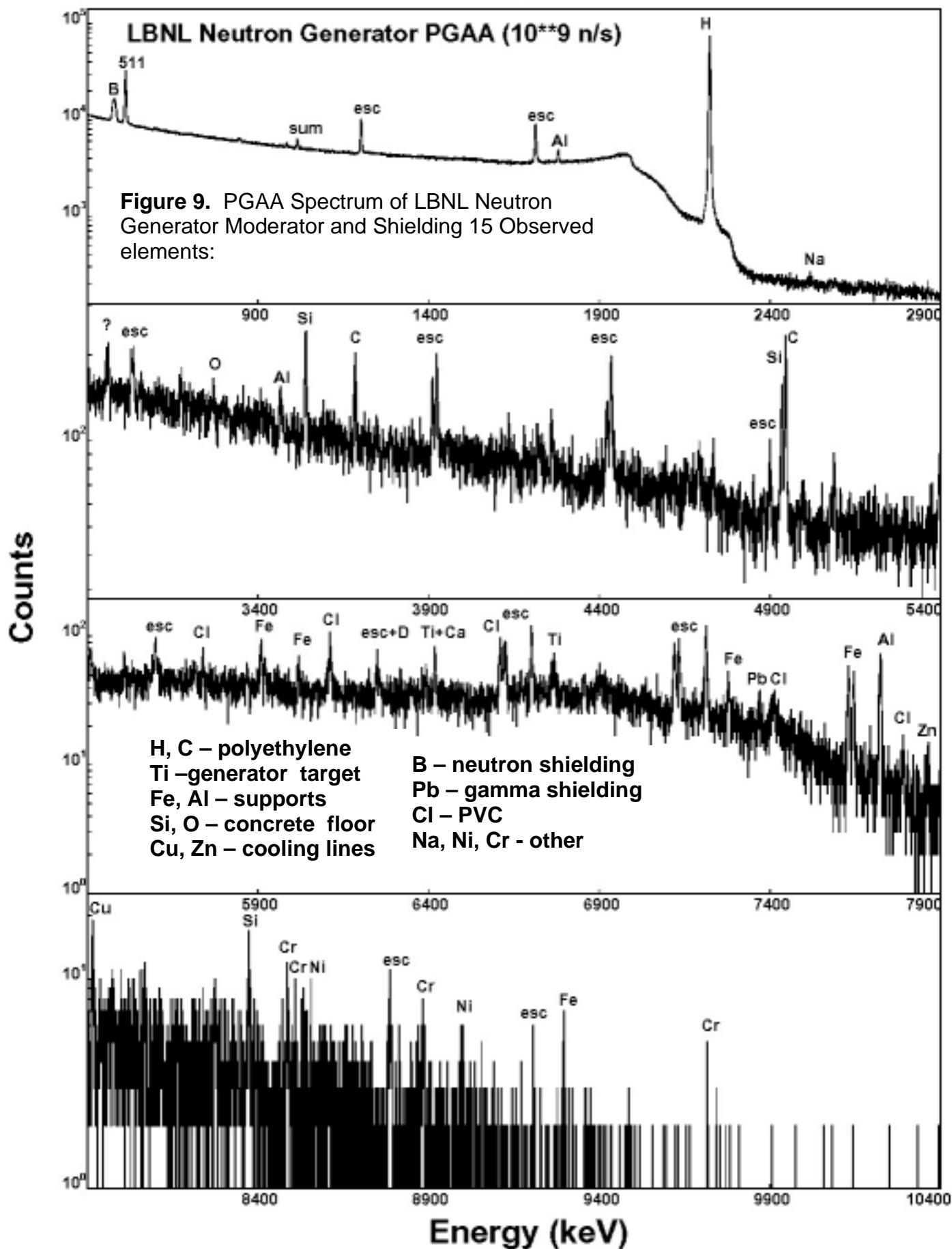


Figure 8. The LBNL neutron facility on the left, the co-axial neutron generator on the right. The polyethylene moderator/shielding are pulled back to show the generator.

A. NAA applications with neutron generators

The maximum thermal neutron flux produced at the LBNL neutron generator was 10^5 n/cm²s measured using 5 cm polyethylene moderator. Although the γ -ray background was very high from the moderator, we were able to see all of the neutron generator components in the PGAA spectrum as indicated in Figure 9. Improved moderator materials and neutron guides would be required to make PGAA a practical application with neutron generators.

Although the neutron generator thermal flux is low, we have found that NAA can be applied successfully for identifying many elements, especially when the capture isotope half-life is short. Figure 10 shows an example for the NAA analysis of cobalt with the LBNL neutron generator. Sensitivity to mg amounts of many materials makes NAA with a neutron generator suitable for bulk analysis of unknown samples.



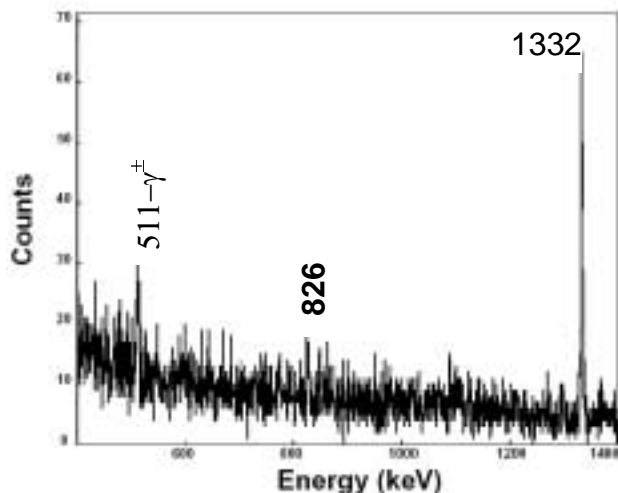


Figure 10. $^{60}\text{Co}^{\text{m}}$ (10.5 min) spectrum. NAA analysis of 1 g sample of cobalt metal bombarded for 10 min and counted for 12 minutes.

B. Fast Neutron Activation Analysis (FNAA) with Neutron Generators

An alternate to NAA analysis with neutron generators is FNAA using fast neutrons without moderation. Nuclear reactions, including (n,n') , (n,p) , (n,α) , and $(n,\text{fission})$ can be used to produce radioactive products for off-line analysis. These cross sections are typically much lower than thermal neutron activation cross sections, but the sample can be placed much closer to the generator increasing the neutron flux by factors of 100-1000. Figure 11 shows the spectrum for analysis of mercury by the $^{199}\text{Hg}(n,n')^{199}\text{Hg}^{\text{m}}$ reaction.

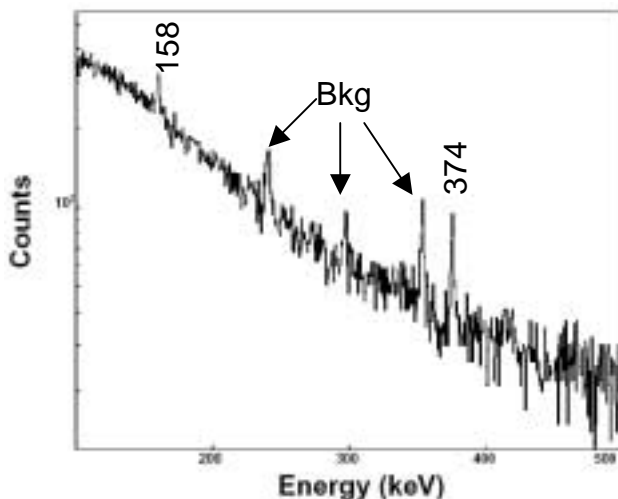


Figure 11. $^{199}\text{Hg}(n,n')^{199}\text{Hg}^{\text{m}}$ (42.6 min) NAA analysis of 50 g sample of HgSO_4 bombarded for 30 min and counted for 30 min.

Another application of FNAA is the detection of uranium by the $(n,\text{fission})$ reaction. This method has been demonstrated with thermal neutrons¹⁸ where the large fission cross section for ^{235}U (582.6 b) compensates for the low abundance (0.72%). This technique requires detection of fast delayed fission neutrons or high-energy decay γ -rays from short-lived fission products. However, quantitative

detection of uranium is problematic as discussed below. Uranium detection with fast neutrons is nearly as effective because the fast neutron induced fission cross-section for $E_n > 2$ MeV ranges from 0.1-1 barns for the abundant ^{238}U . Figure 12 shows an example of the analysis of uranium using high-energy γ -rays, and Figure 13 indicates the background rate of spontaneous fission delayed neutrons from ^{238}U .

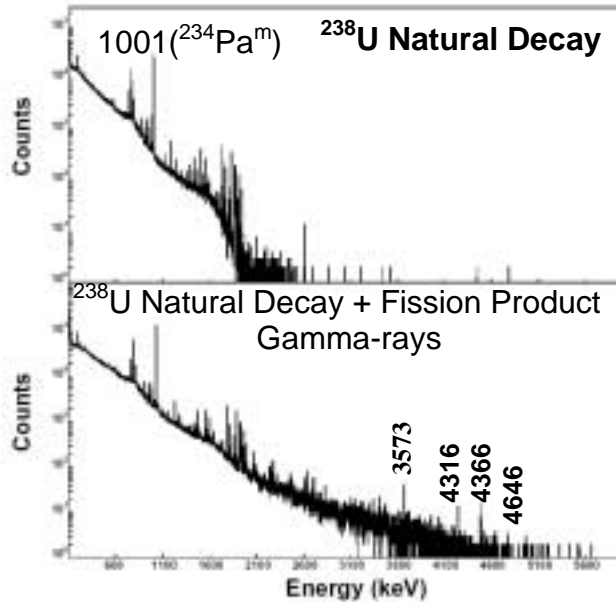


Figure 12. Detection of uranium by high-energy fission product gamma rays. The top spectrum records the decay of depleted uranium counted for one hour, and the bottom spectrum shows the same sample counted for 6 minutes following a 10-minute bombardment. The energies of gamma rays from the decays of $^{90}\text{Rb}^{m+g}$ are indicated.

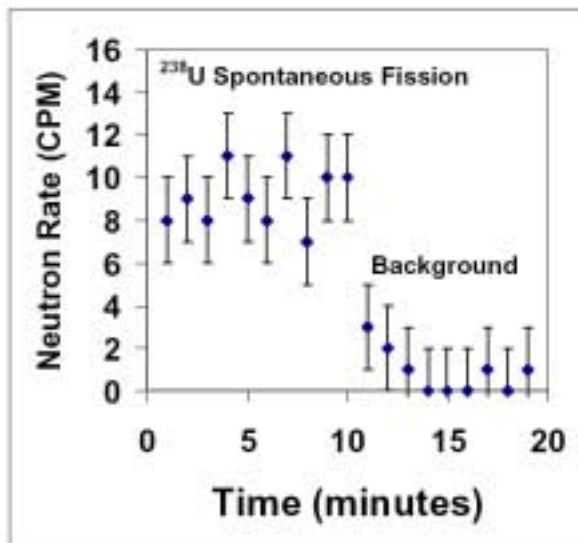


Figure 13. Comparison of background and spontaneous fission rates measured with a ^3He detector 10 cm from 14.65 kg of depleted uranium. ^{238}U spontaneously fissions with a rate of ≈ 6 fissions per second per kg.

C. Quantitative analysis with fast neutrons

Elemental quantitative analysis with fast neutrons is complicated by the lack of a well-calibrated cross section or k_0 database. This is further complicated by the fact that different laboratories may use neutron beams of different energies. The analysis of uranium by detection of high-energy fission product γ -rays was demonstrated to be quantitative by Molnar et al¹⁷ as shown in Figure 14.

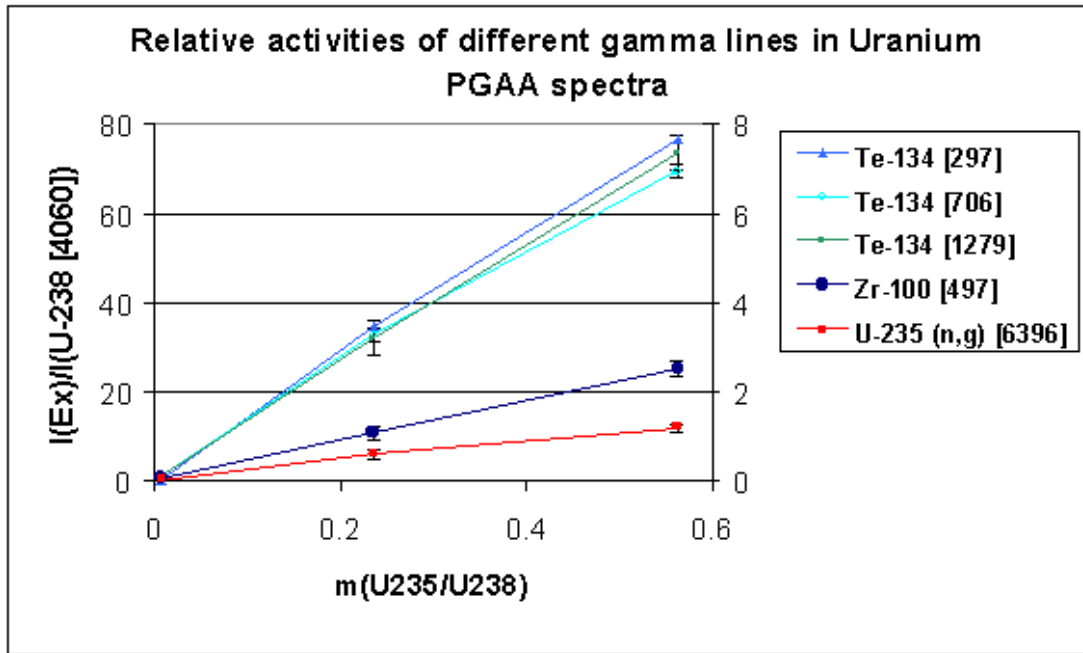


Figure 14. Spectrum of prompt (upper) and fission product decay (lower) gamma rays produced following the irradiation of Uranium, enriched to 36% ^{235}U , with cold neutrons from the Budapest Reactor. The decay spectrum was acquired with a neutron beam chopper set to a 20 ms activation phase and 16 ms counting interval.

The uranium product fission yields are different for fast neutrons, as shown in Table 8 where we compare the analysis of the thermal neutron data from Budapest with the LBNL fast neutron data. Comparison with the standard fission yields from ENDF-349¹⁹ is good for thermal neutrons but poor for fast neutrons.

Table 8. Comparison of measured and semi-empirical fission product gamma ray yields. Cold neutron measurements were performed at the Budapest Reactor and D+D measurements at the Berkeley Neutron Generator Facility. Semi-empirical values were obtained from the compilation of England and Rider (ENDF-349)¹³.

Fission Product	E_γ (keV)	Relative Fission Yields				
		Experiment		ENDF-349		
		$^{235}\text{U(cold)}$	$^{238}\text{U(2.5 MeV)}$	Thermal	Fast	$^{239}\text{Pu(thermal)}$
$^{90\text{m}}\text{Rb(258 s)}$	3317.00(17)	77	145	70	44	33
$^{95}\text{Y(10.3 m)}$	3575.84(20)	147	325	162	226	88
$^{90}\text{Rb(158 s)}$	4135.47(20)	100	100	84	84	84
$^{90}\text{Rb(158 s)}$	4365.82(24)	95	96	100	100	100

Detection of delayed fission neutrons or fission product activity is complicated by induced fission reactions within the target. This was demonstrated in the analysis of the $^{235}\text{U}/^{238}\text{U}$ ratios that I measured in archaeological artifacts from Paleoindian sites²⁰. A summary of our results measured at the McMaster University Reactor is shown in Figure 15.

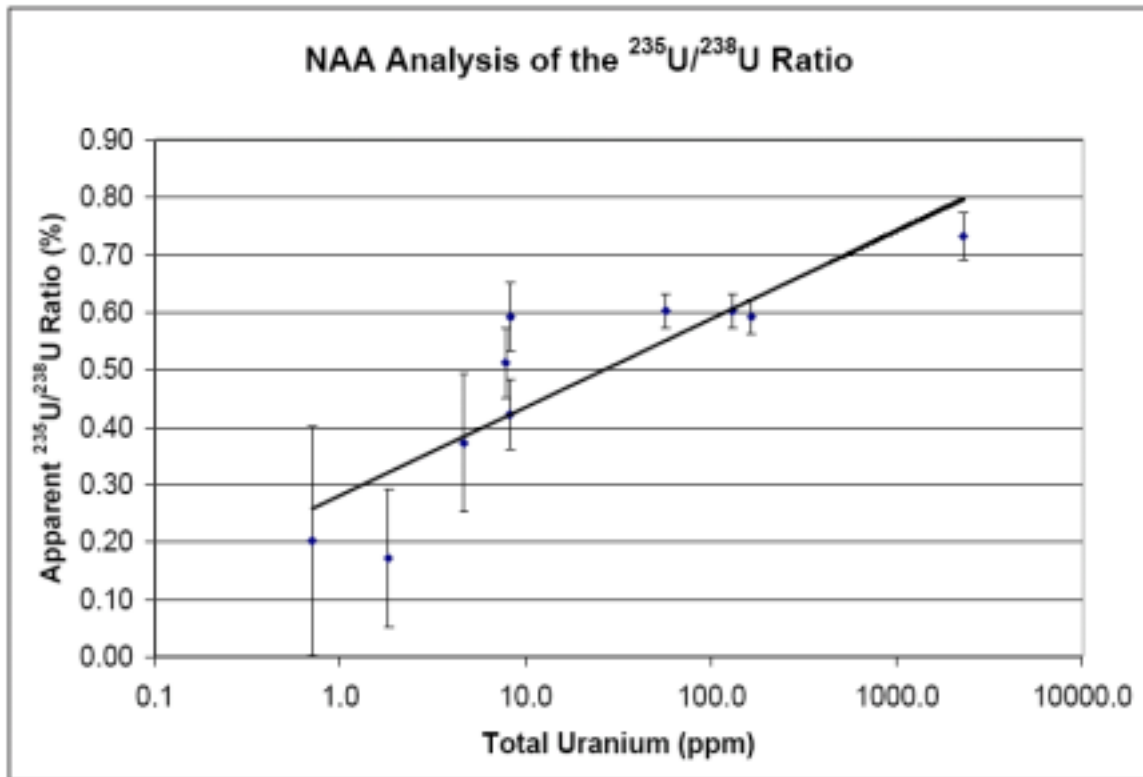


Figure 15. Analysis of $^{235}\text{U}/^{238}\text{U}$ ratio in Paleoindian cherts by NAA. The line is only to guide the eye. The expected ratio is 0.72.

The analysis of ^{238}U was done using NAA and detecting of the $^{239}\text{U} \rightarrow ^{239}\text{Np}$ decay series, and ^{235}U analysis was performed by delayed neutron counting. Note that only the highest concentration Uraninite sample appeared to have the normal ratio of 0.72%. It has been well established that virtually all terrestrial uranium samples have normal $^{235}\text{U}/^{238}\text{U}$ ratios, so these results indicate either extraordinary materials or a subtle mistake in the analysis.

We performed a second analysis of these samples at the USGS using thermal ionization mass spectrometry (TIMS) and measured the results shown in Table 9.

Table 9. Measurements of the $^{238}\text{U}/^{235}\text{U}$ ratios in paleoindian artifacts using TIMS. The normal expected ratio is 137.9.

$^{238}\text{U}/^{235}\text{U}$ ratio measured on chert samples by thermal ionization mass spectroscopy
James L. Bischoff, USGS, analyst, 9 July 2001

Sample	USGS lab no.	$^{238}\text{U}/^{235}\text{U} \pm (1\text{SD})$
Chuska chert	01-140	137.5(1.3)
Onandaga chert	01-141	no U yield
Bayport chert	01-142	138.1(1.0)
Upper Mercer chert	01-143	137.7(3.7)
Fossil Hill chert	01-144	136.6(0.85)
Gainey chert	01-145	137.85(1.6)
Uraninite Std.(HU-1)	01-146	137.81(1.2)

In these measurements all of the samples agreed well with the expected values.

What happened? Note that there is a clear trend of increasing depletion with decreasing concentration. The explanation lies in the fact that thermal neutrons induce additional neutrons by the fission of uranium in the target. If the target has a large uranium concentration, as is the case of the Uraninite standard, then the total effective neutron flux will be higher than when the concentration is lower. More delayed neutrons will be emitted from higher concentration uranium samples, and low concentration samples will appear to be depleted. In our measurements, the method was calibrated with Uraninite and extrapolated to lower concentrations leading to the results we observed.

D. Extension of the EGAF database to fast neutrons.

Few systematic measurements of fast neutron cross sections are available. One exception is the *Atlas of Gamma-ray Spectra from the Inelastic Scattering of Reactor Fast Neutrons*²¹. Reactor energy neutrons with an average energy of 1 MeV were used to irradiate 72 elemental targets from Li to U. Gamma ray spectra were measured for each target, and the analyzed transitions were assigned to their associated reactions. Gamma-ray data were measured on a relative intensity scale for each target, and absolute normalizations with respect to the 847-keV γ -ray in Fe were reported. It will be straightforward to convert the γ -ray intensities into cross sections and k_0 values. We plan to add these data to the EGAF database thus producing the first comprehensive k_0 database for fast neutrons.

¹ G.L. Molnar, Z. Revay, and T. Belgia, Nucl. Instrum. Meth. Phys. Res. A489, 140-159 (2002).

² B. Krusche, K.P. Lieb, H. Daniel, T. von Egidy, G. Barreau, H.G. Nornier, R. Brissot, C. Hofmeyr, and R. Rascher, Nucl. Phys. A386, 245-268 (1982).

³ G.L. Molnar, Z. Revay, R.L. Paul, and R.M. Lindstrom, J. Radioanal. Nucl. Chem. 234, 21-26 (1998).

⁴ Z. Revay, G.L. Molnar, T. Belgia, Z. Kasztovszky, and R.B. Firestone, J. Radioanal. Nucl. Chem. 244, 383-389 (2000).

⁵ Z. Revay, Z. and G.L. Molnar, *Characterization of neutron beam and gamma spectrometer for PGAA*, pp. 57-68 in Summary Report of 2nd Research Coordination Mtg. on Development of a Database for Prompt Gamma-ray Activation Analysis, INDC(NDS)-424, International Atomic Energy Agency, Vienna, 2001.

⁶ R.B. Firestone, Z. Revay, and G.L. Molnar, *New capture gamma-ray library and atlas of spectra for all elements*, pp. 507-513 in Proc. 11th Int. Symp. Capture Gamma-Ray Spectroscopy and Related Topics, J. Kvasil, P. Cejnar, M. Krticka, (Eds.), World Scientific, Singapore, 2003.

⁷ G.L. Molnar, Z. Revay, T. Belgya, and R.B. Firestone, *Appl. Radiat. Isot.* 53, 527-533 (2000).

⁸ Z. Revay, G.L. Molnar, T. Belgya, Z. Kasztovszky, and R.B. Firestone, *J. Radioanal. Nucl. Chem.* 248, 395-399 (2001).

⁹ Z. Revay and G.L. Molnar, *Standardisation of the prompt gamma activation analysis method*, *Radiochim. Acta* (in press).

~~[10]~~¹⁰ RÉVAY, Z., MOLNÁR, G.L., BELGYA, T., KASZTOVSZKY, Z., In-beam determination of k_0 factors of short-lived nuclides, *J. Radioanal. Nucl. Chem.* (in press).

¹¹ *Database of Prompt Gamma rays from Slow Neutron Capture for Elemental Analysis*, R.B. Firestone, H.D. Choi, R.M. Lindstrom, G.L. Molnar, S.F. Mughabghab, R. Paviotti-Corcuera, V. Zerkin, and Zhou, IAEA RECD0C, in press.

¹² Evaluated Nuclear Structure Data File, a computer file of evaluated experimental nuclear structure data maintained by the National Nuclear Data Center, Brookhaven national laboratory, USA.

¹³ Evaluated Nuclear Structure Data File, a computer file of evaluated experimental nuclear structure data maintained by the National Nuclear Data Center, Brookhaven national laboratory, USA.

¹⁴ R.B. Firestone, V.S. Shirley, C.M. Baglin, S.Y.F. Chu, and J. Zipkin, *8th edition of the Table of Isotopes*, John Wiley & Sons, New York (1996).

¹⁵ *Table of radionuclides*, M.-M. Bé, V. Chisté, C. Dulieu, E. Browne V., Chechev N. Kuzmenko R., Helmer A. Nichols E. Schönfeld and R. Dersch, monograph by the Bureau International des Poids et Mesures (BIPM) on behalf of the Comité Consultatif des Rayonnements Ionisants (CCRI), previously known as the Comité Consultatif pour les Étalons de Mesure des Rayonnements Ionisants (CCEMRI).

¹⁶ S.F. Mughabghab, M. Divadeenam, and N. Holden, *Neutron Cross Sections*, Vol. 1, Part A, Z = 1-60, Academic Press, New York, 1981.

¹⁷ Compact Neutron Generator Development at LBNL, J. Reijonen, G. English, R. Firestone, F. Giquel, M. King, K-N. Leung, M. Sun, *Proceedings of the American Nuclear Society 2003 Annual Meeting*, June 1-5 2003, San Diego CA., p 579, Accelerator Applications 2003 (ANS Publishing, Chicago, 2004).

¹⁸ G.L. Molnár, Zs. Révay, T. Belgya, *Non-destructive Interrogation of Uranium using PGAA*, *Nucl. Instrum. Methods B213* (2004), 389-393.

¹⁹ T.R. England, B.F. Rider, *Evaluation and Compilation of Fission Product Yields*, ENDF-349, LA-UR-94-3106.

²⁰ R.B. Firestone and W. Topping, *Terrestrial Evidence of a Nuclear Catastrophe in Paleoindian Times*, *Mammoth Trumpet* 16, 9 (2001).

²¹ *Atlas of Gamma-ray Spectra from the Inelastic Scattering of Reactor Fast Neutrons, Part 1 ($Z \leq 42$)* M.R. Ahmed, S. Al-Najjar, M.A. Al-Amili, N. Al-Assafi, N. Rammo, A.M. Demidov, L.I. Govor, and Yu. K. Cherepantsev; *Part 2 ($Z \geq 44$)* A.M. Demidov, L.I. Govor, Yu. K. Cherepantsev, M.R. Ahmed, S. Al-Najjar, M.A. Al-Amili, N. Al-Assafi, and N. Rammo, Atomizdat, Moscow (1978).